Available online at www.sciencedirect.com
SCIENCE DIRECT®
International Journal of Heat and Mass Transfer 47 (2004) 5313–5322
International Journal of HEAT and MASS TRANSFER
www.elsevier.com/locate/ijhmt

Analysis of a transient heat transfer experiment in a two pass internal coolant passage

D. Chanteloup [a], J. von Wolfersdorf [b,*]

[a] Ecole Polytechnique Fédérale de Lausanne (EPFL), Laboratoire de Thermique appliquée et de Turbomachines (LTT), 1015 Lausanne, Switzerland
[b] Institute of Aerospace Thermodynamics, University of Stuttgart, Pfaffenwaldring 31, 70569 Stuttgart, Germany

Received 14 October 2003; received in revised form 14 May 2004
Available online 20 August 2004

Abstract

A study of heat transfer in a two-pass internal cooling passage of gas turbine airfoils is presented. Heat transfer measurements were performed with a transient technique using thermochromic liquid crystals. Flow temperature measurements along the channels are used to evaluate the heat transfer distribution. Thereby two methods are applied. The first uses the measured temperature histories directly and applies the superposition method for data evaluation. The second method analyses first the fluid temperature data using a simplified model and relates them to the average flow temperature at a given location. The results of both methods are compared.

Keywords: Heat transfer; Measurement techniques; Transient

1. Introduction

Transient heat transfer measurement techniques using thermochromic liquid crystals (TLC) have been used extensively in obtaining detailed heat transfer distributions in model passages of gas turbine airfoils. Good reviews on this technique are given e.g. by Ireland and Jones [1] and Ekkad and Han [2]. Many coolant passages for gas turbine blades consist of two pass configurations connected by a 180° bend. Therefore such configurations have been studied in several investigations (e.g. [3–8] among others). For transient measurements in long internal cooling channels the fluid temperature varies with stream-wise position and time. Usually a series of thermocouples is installed along the flow path and the measured time histories are analysed as a series of steps using the superposition method [9,2]. Several approaches have been developed to relate the measured fluid temperature to the average mean or the bulk temperature at the specific location. Chyu et al. [10] presented various strategies for analysing the measurement data based on stream-wise energy balances, as introduced by Metzger and Larson [9], for the non-isothermal wall situation. A concept based on an invariant local heat flux with time was found to be superior to other data evaluation techniques.

* Corresponding author. Tel.: +49 711 685 2316; fax: +49 711 685 2317.
E-mail addresses: denis.chanteloup@turbomeca.fr (D. Chanteloup), jens.vonwolfersdorf@itlr.uni-stuttgart.de (J. von Wolfersdorf).

0017-9310/$ - see front matter © 2004 Elsevier Ltd. All rights reserved.
doi:10.1016/j.ijheatmasstransfer.2004.06.026

Nomenclature

A	parameter
c_p	specific heat at constant pressure
D_h	hydraulic diameter
h	heat transfer coefficient
H	heat transfer parameter
k	wall material property $k = \sqrt{\lambda \rho c_p}$
m	mass flow rate
Nu	Nusselt number
P	perimeter
Pr	Prandtl number
Re	Reynolds number
t	time
T	temperature
U_b	bulk velocity
x	stream-wise position measured from entrance
$\overline{X}$	axial coordinate in bend region
$\overline{Z}$	vertical coordinate in bend region
γ	profile factor
λ	thermal conductivity
v	viscosity
ρ	density
ξ	axial coordinate measured from entrance
Θ	dimensionless temperature

Subscripts

E	entrance or inlet
f	fluid average
i	initial
LC	liquid crystal
s	equivalent isothermal solid wall
TC	thermocouple
W	wall
0	reference value

A simplified analytical model for the fluid temperature development was used by von Wolfersdorf et al. [11] under the assumption of an equivalent isothermal upstream wall situation for each instant. This assumption was introduced earlier by Gillespie et al. [12]. A numerical analysis for this condition was applied by Tsang et al. [13] and experimentally verified for smooth and ribbed cooling channels. It was found, that for well-mixed flow situations as for e.g. turbulated cooling channels, a single thermocouple located near the channel core can be used with confidence for the data evaluation. Another approach was used by Schubert et al. [14] using numerical simulations to derive a relationship between the bulk temperatures and the measured temperatures at the channel centreline.

The current work will compare two approaches for the data analysis of heat transfer experiments in a two pass internal cooling channel with an inclined bend, similar to the configurations given in Chanteloup et al. [15] and Chanteloup and Bölcs [16]. First the measured local temperature histories are used and the superposition method is applied. Then an analytical model using a simplified one-dimensional quasi-steady energy balance as given in [11] is used and the thermocouple data analysed to obtain physical parameters describing the fluid temperature behaviour. With this method the reference fluid temperature is corrected towards the fluid bulk temperature at the respective location and erroneous temperature readings can easily be identified. Further, using this method, a closed form solution for the wall temperature response can be used to determine the local heat transfer coefficients, which is finally compared to the data from the first method.

2. Experimental setup

For the present experiments, air was the working fluid and was supplied by a continuously running compressor. The air enters the settling chamber with an inner diameter of 600 mm via a 150 mm tube and a conical entrance section with an angle of 30°. The settling chamber is equipped with a combination of perforated plates, honeycombs and meshes to reduce unsteadiness and swirl in the flow. A bell mouth entry leads the air from the settling chamber to the test channel. The settling chamber outlet is equipped with fine mesh heaters for the heat transfer measurements. The facility was used to perform heat transfer and flow measurements. The three-dimensional velocity fields at several positions were obtained using a particle image velocimetry (PIV) measurement method. Details on the PIV setup and the flow results can be found in [4,15,16]. During the flow measurements, the heaters are removed from the channel. A turbulence grid is placed downstream of the heaters in both flow and heat transfer measurements to reach the same turbulence level at the channel inlet.

A sketch of the test section is shown in Fig. 1. The overview of Fig. 1 shows the baseline configuration already described in previous work, see Chanteloup et al. [15]. The channel is a 2-pass channel with 45° ribs in a staggered arrangement, with rib heights of 0.15 hydraulic diameters, and rib spacing of 10 rib heights. The particular test section for the present study is shown in Fig. 1 details. It is a two-pass cooling passage model of a gas turbine blade. The flow path in the downstream and upstream passages has a cross-section of $100 * 100$ mm^2

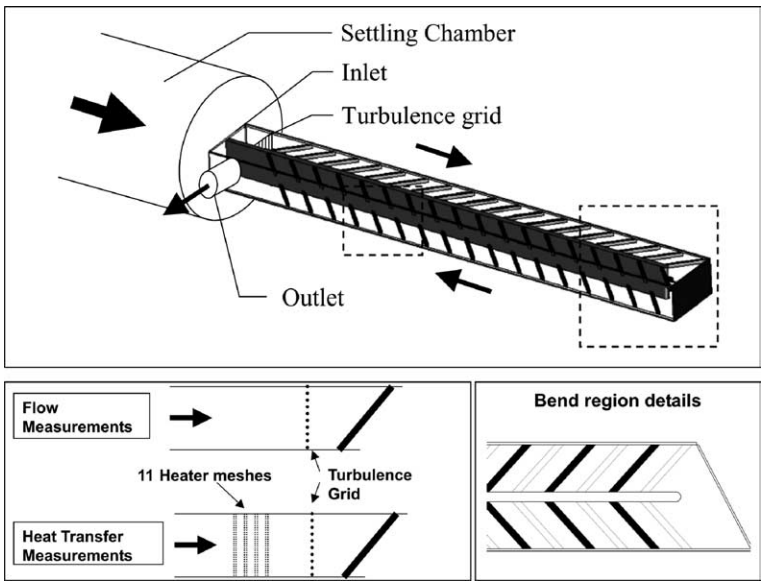

Fig. 1. The internal coolant passage test facility and inlet region details.

with a corresponding hydraulic diameter $D_h = 100$ mm and a length of $20D_h$. The outer walls of the test section are made of extruded Plexiglas to obtain good optical properties. In the straight-corner bend, the clearance between the tip of the divider plate and the outer wall is equal to D_h. The thickness of the divider plate or web between the two passages is $0.2D_h$. The tip of the divider plate is cylindrically shaped with a $0.1D_h$ radius. Square ribs with an angle of 45° to the passage centreline, rib heights of 0.15 hydraulic diameters, and rib spacing of 10 rib heights are mounted in a staggered arrangement on the top and bottom wall of the passage. The ribs in the bend region and the configuration of the bend are shown in Fig. 2. Eleven ribs are mounted on each of the top and bottom walls in each of the upstream and downstream passages of the model. The turn region end wall is inclined 30° from the upstream centreline.

The measurements were obtained with air as working fluid, at a flow Reynolds number of 70,000 (corresponding to a bulk velocity of 10.61 m/s) at the entrance of the test section. The Reynolds number is based on the 0.1 m hydraulic diameter and on the mean axial velocity at the entrance of the channel. Upstream of the test section, the mass flow is measured by means of a flow meter with a 1% accuracy. The turbulence level is approximately 3% at the inlet of the test section.

The definition of the coordinate systems in the bend region is shown in Fig. 2. The origin of the coordinate system is set on the bottom wall at the centre of the rounded end of the web, which is 20 hydraulic diameters downstream of the heater mesh. At the indicated cross-section flow field measurements using particle image velocimetry (PIV) and temperature measurements were performed using eight thermocouples located as given in Fig. 3.

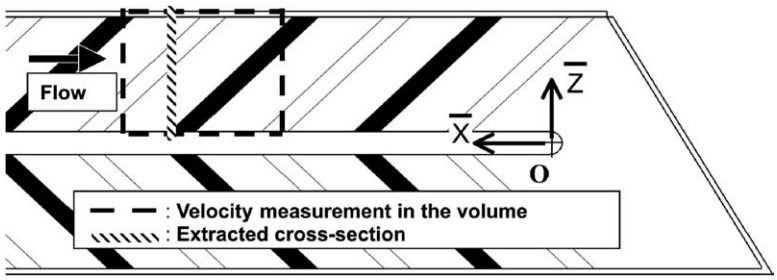

Fig. 2. Coordinate system in the bend region.

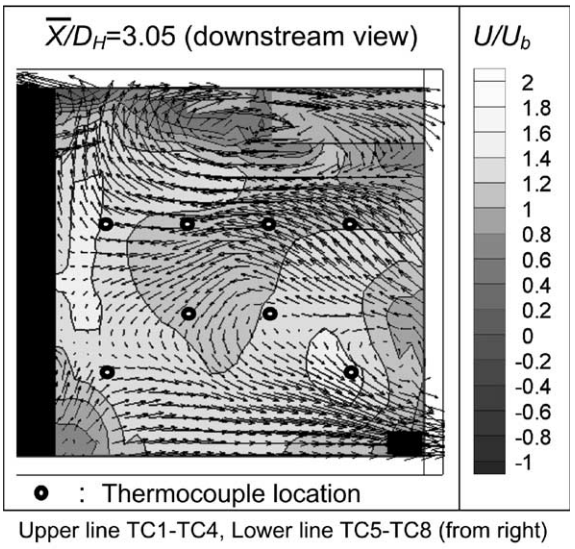

Fig. 3. Stream-wise velocity distribution and secondary flow field at extracted cross-section.

3. Measurement technique

For the present study, transient heat transfer experiments were performed using liquid crystals to determine the surface temperature. The transient liquid crystal technique consists of monitoring the surface temperature indication with time using a step change in the gas temperature at the inlet. Eleven fine, fast response, mesh heaters were fitted to the duct inlet to produce the step change in gas temperature. These heaters comprise a mesh of stainless steel wires, 40 μm in diameter woven at a pitch of approximately 100 μm, with an open area of 38% (see Wang et al. [17]). The meshes were connected in series to a 10 kW power supply (256 A, 40 V). At the inlet, the heaters provide a step change in temperature of 75% and 99% of the total temperature increase, in 0.4 and 0.6 s, respectively. The temperature distribution across the inlet section was measured with eight thermocouples and the variation between them was found to be less than 3%.

The transient heat transfer measurement method consists of monitoring the surface temperature evolution by acquiring the colour signal of a liquid crystal coating applied on the walls of the test section. By using a single layer of narrow-band thermochromic liquid crystals (Hallcrest BM/R30.5C0.7W/C17-10), the indication of the local surface temperature $T_W(t_{indication}) = T_{LC}$ is obtained from a hue capturing technique. Several miniature colour CCD cameras, mounted around the test section, record the colour change of the liquid crystal coating. The video signal of each view is digitally stored on DV (Digital Video) tapes. The use of the DV format storage ensures precise colour image signal restitution at constant image frequency without any noise generation. Video sequences of each camera are transferred subsequently to a computer, where the image processing and the data reduction are performed.

The liquid crystals are painted directly on the channel inner Plexiglas surface. A black paint coating covers the liquid crystals to provide a good background for image acquisition. Therefore measurement information are obtained only between the ribs. In a gas turbine blade application an additional cooling effect due to the thermally active ribs would be present. Thermocouples were placed along the channel to measure the local gas temperature. They were located in the centre of one of the secondary flow vortex induced by the ribs. Tests based on numerical simulations, showed that at this cross-section location the gas temperature is closer to the bulk temperature than the centreline temperature. The thermocouples were separated 1.5 hydraulic diameters from each other in the region of interest. A linear interpolation of the gas temperature in stream-wise direction was performed for every location between the thermocouples.

Due to the length of the test section the gas temperature is a function of time and stream-wise location. Downstream of the inlet, due to heat exchange, the temperature increase is no longer a step. For a given position, the gas temperature is an increasing function of time. It can be shown, that, when the gas temperature change can be expressed as a series, the surface temperature $T_W(t)$ is (see e.g. [2])

$$T_W(t) - T_i = \sum_{j=1}^{N} \left[1 - \exp\left(\frac{h^2(t-t_j)}{k}\right) \times \operatorname{erfc}\left(\frac{h\sqrt{t-t_j}}{\sqrt{k}}\right) \right] \Delta T_{m(j,j-1)} \quad (1)$$

where ΔT_m and t_j are the temperature and time step changes obtained from the temperature histories of the thermocouples. An iterative procedure is therefore required to determine the values of the heat transfer coefficients.

The error in the heat transfer measurements has been calculated considering the method described by Höcker [18]. It showed, that the error can be minimised by adjusting measurement parameters as the model material properties and the dimensionless temperature $\Theta_W = \frac{T_W(t)-T_i}{T_E-T_i}$. In the present study, the heat transfer coefficients are of the order of 20–200 W/(m^{2}K) and the wall material is Plexiglas. Using the method of Höcker [18], this leads to optimum dimensionless temperatures between $0.2 < \Theta_W < 0.4$. Two tests have been performed with inlet temperatures T_E of 62.1 and 71.1 °C at model initial temperatures T_i of 17.8 and 16.9 °C for test 1 and test 2, respectively. Therefrom, the maximum error was estimated to ±8% on the heat transfer coefficient under the assumption that the heat transfer coefficient is constant during the experiment.

4. Results

Fig. 3 shows the measured velocity distribution in the fully developed region at the extracted cross-section (see Fig. 2). This velocity distribution is typical for a cooling channel with 45° ribs, where the vortices behind inclined ribs move along the ribs and then join the main flow. This interaction between main flow and rib-induced vortices causes a strong secondary motion in the passage. The secondary flow consists of two counter-rotating vortices that push fluid from the duct center towards the web along the center plane and to the sidewall along the ribbed walls as shown in Fig. 3. It was shown by Chanteloup [4], that the secondary flow field impinges on two main areas in the channel. Secondary flow with velocities as high as 30% of the bulk velocity impinges on the outer wall at approximately one rib height above the ribbed wall. Flow with lower velocities (about 10% of the bulk velocity) impinges on the web among the center plane. These velocity distributions cause different heat transfer patterns on the channel walls. Fig. 3 indicates further the location of eight thermocouples in the cross-section which were used for the data evaluation with a simplified analytical model given later.

Fig. 4 shows the full surface heat transfer distribution on all walls of the configuration in the region of interest. The data are given as normalized Nusselt numbers using

$$Nu_0 = \frac{h_0 D_h}{\lambda} = 0.023 Re^{0.8} Pr^{0.4} \tag{2}$$

where $Re = U_b D_h / v$ as a reference value for a smooth channel.

On the bottom wall upstream of the bend, the heat transfer distribution is typical for a periodic flow behaviour in channels with 45° rib arrangements. The heat transfer distribution is repetitive from one rib module to another. In the last rib module upstream of the bend, the region of high heat transfer is more angled than in the other rib modules, indicating the influence of the bend region. The secondary flow caused by the ribs dominates the heat transfer distribution until the flow has entered the bend itself. The bend region heat transfer distribution is different than in the ribbed region. No high heat transfer gradients occur compared to the upstream ribbed region. The upstream fully developed distribution shape is recovered from the first rib module downstream of the bend. The upstream leg level and shape are reached after 5 hydraulic diameters downstream from the bend. On the top wall, the upstream heat transfer distribution is similar to the one of the bottom wall. This can be attributed to the symmetrical shape of the secondary flow field about the centre plane.

On the downstream sidewall near the bend, $0 < \overline{X}/D_h < 3$, the heat transfer coefficients are higher than in the downstream region. This increase is attributed to the flow acceleration as the flow from the bend impinges on the sidewalls. Further downstream, the heat transfer reaches the upstream inner sidewall periodic flow developed values.

Note that these heat transfer distributions are different from the bottom wall to the top wall and are not symmetrical. First, the U-shaped high heat transfer region downstream of the rib is more shifted towards the downstream direction on the top wall than on the bottom wall. This is due to the size of the recirculating vortex induced by the ribs, which is bigger behind ribs on the top than on the bottom wall. Second, no high heat transfer region occurs on the top wall at the location

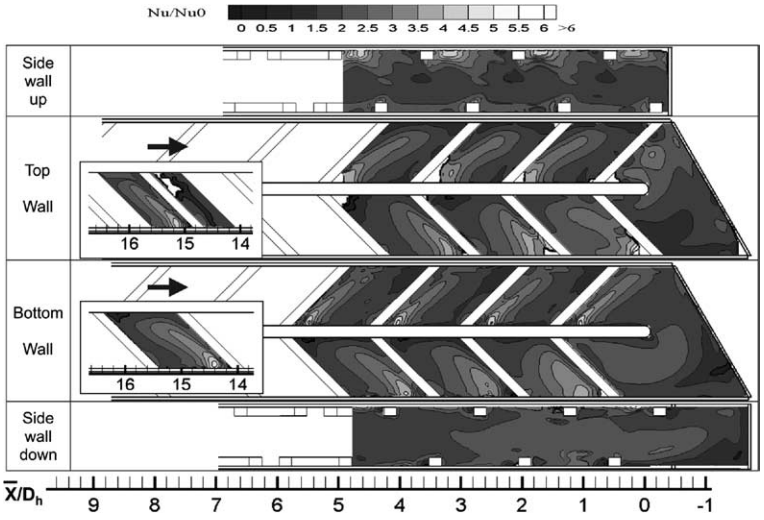

Fig. 4. Detailed heat transfer distribution in the channel.

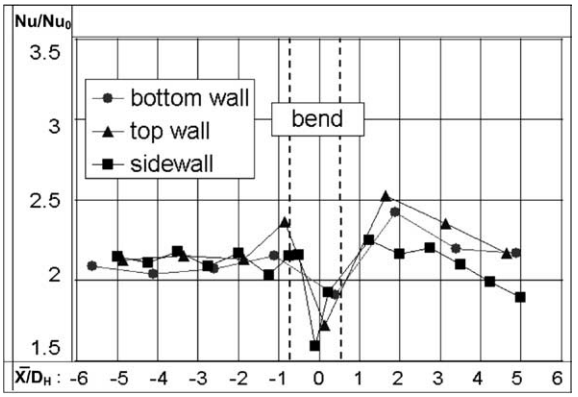

Fig. 5. Average heat transfer distribution along the channel.

of the vortex impact on the sidewall. This is due to the weak impact of the rib-induced vortex on the top wall. Furthermore, these full surface differences give an explanation of the 4% difference between both ribbed wall area averaged values. Fig. 5 shows the area averaged heat transfer distribution along the channel. The general trend of the heat transfer distribution can be summarized as follows. On the ribbed walls, the values of Nu/Nu_0 are nearly constant in the upstream leg, indicating that the flow is periodically developed. The value remains the same up to 1.5 hydraulic diameters upstream of the bend. The ribbed wall Nu/Nu_0 values are strongly influenced in the bend itself, with an increase of heat transfer of 10% in the upstream part of the bend and a decrease of up to 20% in the downstream part of the bend. Downstream of the bend, the ribbed wall values first increase to levels as high as 2.5, and farther recover from the bend effect.

The side wall heat transfer distribution is different from the ribbed wall distribution. It undergoes the bend effect further upstream of the bend. Downstream of the bend, the Nu/Nu_0 values decrease to levels lower than in the upstream leg.

5. Alternative method for data evaluation

An alternative approach for the data evaluation was taken to analyse the obtained experimental data using simplified analytical modelling. A shown by von Wolfersdorf et al. [11], the principle behaviour of the mass averaged fluid temperature at a given location can be described for the transient experiments by

$$\Theta_{\mathrm{f}} = \frac{T_{\mathrm{f}}(x,t) - T_{\mathrm{i}}}{T_{\mathrm{E}} - T_{\mathrm{i}}} = 1 - \left(1 - \exp\left(-\frac{HP}{mc_p}x\right)\right) \times \exp\left(\frac{H^2A^2t}{k}\right)\mathrm{erfc}\left(\frac{HA\sqrt{t}}{\sqrt{k}}\right) \tag{3}$$

where

$$A = \frac{1 - \exp\left(-\dfrac{HP}{mc_p}x\right)}{\dfrac{HP}{mc_p}x} \tag{4}$$

and H is an upstream heat transfer parameter, which is defined from a one-dimensional energy balance as (see [11] for details)

$$H(x) = \frac{\int_0^x h(\xi)T_{\mathrm{f}}(\xi,t)\mathrm{d}\xi}{\int_0^x T_{\mathrm{f}}(\xi,t)\,\mathrm{d}\xi} \tag{5}$$

In Eq. (5) ξ is the local axial coordinate measured from the channel entrance. Eq. (3) relates the local average fluid temperature history to the channel entrance temperature under the assumption of an equivalent isothermal upstream wall at any instant. This time varying upstream wall temperature is used as a model, to achieve the local fluid temperature history typically for a transient experiment under isothermal boundary conditions. As shown experimentally by Tsang et al. [13], this model assumptions works well for smooth and ribbed channels. From the simplified analysis presented in [11] the equivalent isothermal upstream wall temperature can be described by

$$\frac{T_{\mathrm{S}}(x,t) - T_{\mathrm{i}}}{T_{\mathrm{E}} - T_{\mathrm{i}}} = 1 - \exp\left(\frac{H^2A^2t}{k}\right)\mathrm{erfc}\left(\frac{HA\sqrt{t}}{\sqrt{k}}\right) \tag{6}$$

where for each stream-wise position x

$$T_{\mathrm{s}}(x,t) = \frac{\int_0^x h(\xi)T_{\mathrm{W}}(\xi,t)\mathrm{d}\xi}{H(x)x} \tag{7}$$

Using this model, each measured fluid temperature history can be described using Eq. (3) with an appropriate heat transfer parameter H at the respective position. With this, the fluid temperature can be used as a boundary condition for the transient conduction problem in the semi-infinite wall model and the local wall temperature response is given by [11]

$$\begin{aligned}\Theta_{\mathrm{W}} &= \frac{T_{\mathrm{W}}(x,t) - T_{\mathrm{i}}}{T_{\mathrm{E}} - T_{\mathrm{i}}} \\ &= 1 - \exp\left(\frac{h^2t}{k}\right)\mathrm{erfc}\left(\frac{h\sqrt{t}}{\sqrt{k}}\right) \\ &\quad + \left(1 - \exp\left(-\frac{HP}{mc_p}x\right)\right)\left(\frac{1}{A\frac{H}{h} - 1}\right)\cdot\left(\exp\left(\frac{H^2A^2t}{k}\right)\right. \\ &\quad \left.\times\,\mathrm{erfc}\left(\frac{HA\sqrt{t}}{\sqrt{k}}\right) - \exp\left(\frac{h^2t}{k}\right)\mathrm{erfc}\left(\frac{h\sqrt{t}}{\sqrt{k}}\right)\right)\end{aligned} \tag{8}$$

Eq. (8) can then be used to determine the local heat transfer coefficients h from the liquid crystal temperature indications.

The first step in the data analysis is the determination of the heat transfer parameter H at the stream-wise positions using Eq. (3). Therefore, the local thermocouple

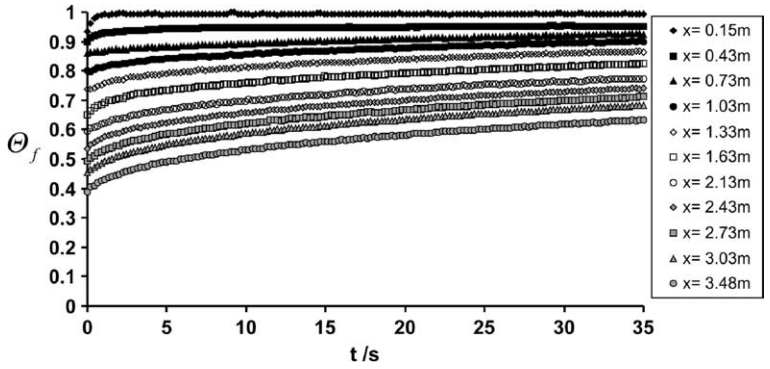

Fig. 6. Fluid temperature histories along the test channel.

measurements have been transformed to the dimensionless temperature Θ_f for the two tests with different temperature settings. The response time of the heater mesh as given above was taken into account using $\Theta_f = \frac{T_f(x,t)-T_i}{T_E(t)-T_i}$. With this, the local temperature histories are related to a step change in the inlet temperature. Both data sets agree very well in this dimensionless form as suggested by Eq. (3). The obtained time distribution at the stream-wise measurement locations is shown in Fig. 6. As it can be seen, the dimensionless fluid temperature drops by more than 30% during the flow through the channel within the measurement period. Using these measurements and Eq. (3) to match the full time history by adapting the heat transfer parameter, it was found, that for some of the thermocouples the measured data did not follow the analytical description satisfactorily. Since Eq. (3) should reflect the average fluid temperature at a given position, this is caused by the fact, that the measured thermocouple temperature is a local temperature at the respective position and not the average fluid temperature. Introducing a profile factor related to the equivalent isothermal upstream wall temperature at any instant

$$\gamma = \frac{T_f(x,t) - T_S(x,t)}{T_{TC}(x,t) - T_S(x,t)} \tag{9}$$

where $T_{TC}(x,t)$ is the measured local temperature history at the respective location. Taking into account Eqs. (3) and (6), the time behavior for the local temperature can be given as

$$\frac{T_{TC}(x,t) - T_i}{T_E - T_i} = 1 - \left(1 - \frac{1}{\gamma}\exp\left(-\frac{HP}{mc_p}x\right)\right) \times \exp\left(\frac{H^2A^2t}{k}\right)\mathrm{erfc}\left(\frac{HA\sqrt{t}}{\sqrt{k}}\right) \tag{10}$$

This equation describes the behaviour very well adapting both, the heat transfer parameter H and the profile factor γ. Thereby it is assumed, that the profile factor is independent of time as it was experimentally demonstrated by Tsang et al. [13]. An illustrative example for the obtained curve fits at one position (x = 1.33 m) using Eqs. (3) and (10) is given in Fig. 7a and b.

Taking the profile factor into account provides a much better match to the measurements. Further, the obtained heat transfer parameter is in the range of the expectations, since although not the same it should reflect the upstream average heat transfer at all walls.

To investigate this behaviour eight thermocouples were placed at one stream-wise position (see Fig. 3). Fig. 8 shows measured temperature histories at this location. There are two "groups" of thermocouples

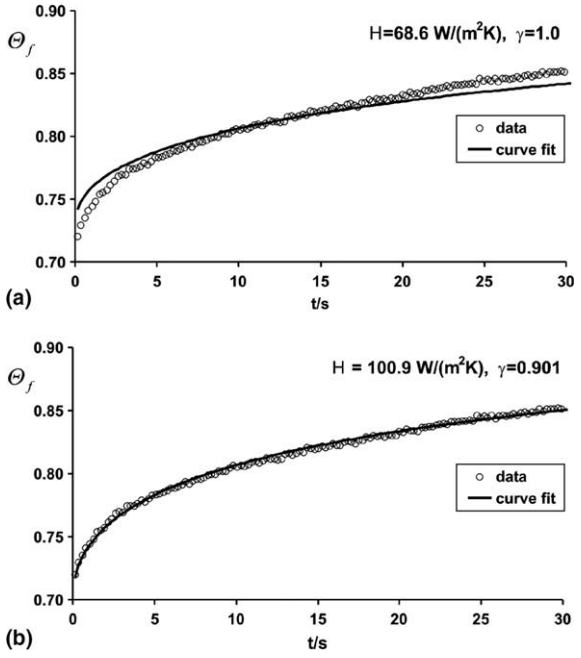

Fig. 7. (a) Curve fit of local fluid temperature history using Eq. (3) and (b) curve fit of local fluid temperature history using Eq. (10).

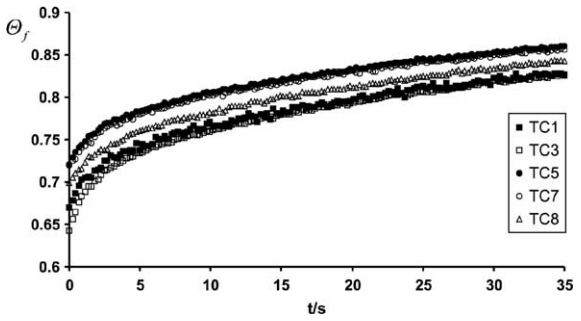

Fig. 8. Dimensionless fluid temperature distributions at extracted cross-section.

indicating higher and lower temperatures respectively. This behaviour can be attributed to the secondary flow field at this location as shown in Fig. 4. The result is a temperature variation of up to 2 K at this location. This will lead to a varying profile factor for the individual thermocouples. The time behaviour for all eight thermocouples is very similar, reflecting a similar heat transfer parameter. All thermocouples have been matched against Eq. (10) to determine H and γ. The result for the two tests is given in Fig. 9.

There is some trend in the obtained data with higher heat transfer parameters relating to lower profile factors. The heat transfer parameter scatters around 10%, which means, that the several wall areas at this location reflect somewhat different equivalent upstream isothermal walls, but agrees well between the two tests. Similar findings were reported by Tsang et al. [13]. The scatter might also be attributed to measurement uncertainties and some non-uniformity in the fluid temperature from the heater mesh. The obtained profile factors reflect the difference in measured fluid temperatures. Profile factors larger than one indicate lower temperatures, and profile factors less than one higher temperatures than the fluid average temperature. Therefrom an approximation can be made for the average fluid temperature using the obtained heat transfer parameter for a given thermocouple and setting $\gamma = 1$ in Eq. (10). The temperature history will therefore be corrected towards the average fluid temperature, although it will not describe this temperature exactly. Investigating the difference in maximum und minimum temperatures measured at this location and comparing this to the values obtained from Eq. (10) by using the maximum and minimum heat transfer parameter at this location and $\gamma = 1$, reduces the difference as given in Fig. 10. The data analysis procedure was applied to the measured thermocouple temperatures along the channel (see Fig. 6). The obtained heat transfer parameters from the two tests are given in Fig. 11. The obtained heat transfer parameters agree within 4% between the two tests. Further, they reflect the expected average heat transfer distribution in the channel with increasing values in the first pass towards the bend and fairly constant values in the second pass. The value near the flow exit is therefore a measure for the full average heat transfer of the configuration (see [19]).

The obtained distribution for the heat transfer parameter was used to evaluate the local heat transfer coefficients using the TLC indications and Eq. (8). Thereby linear interpolation along the channel has been applied. Fig. 13 shows the determined local heat transfer map in the region 1.48 m $< x <$ 2.58 m ($-1 < \overline{X}/D_h < 5$ for the first and the second pass). This distribution is

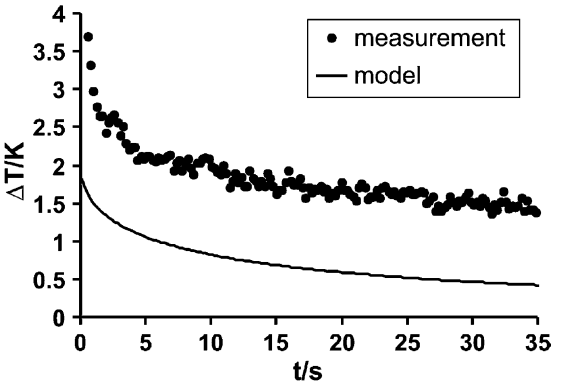

Fig. 10. Maximum difference of local thermocouple data from measurement and model.

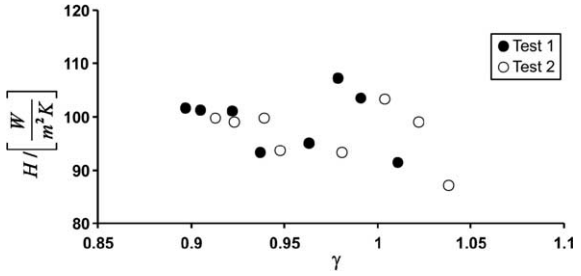

Fig. 9. Variation of heat transfer parameter and profile factor at considered position.

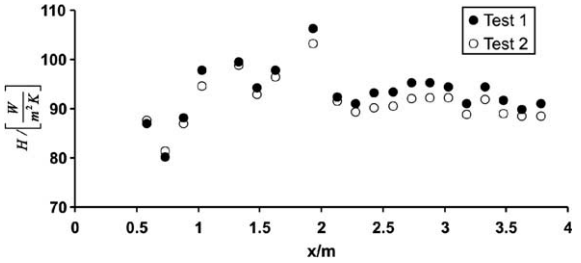

Fig. 11. Obtained distribution of heat transfer parameters along the channel.

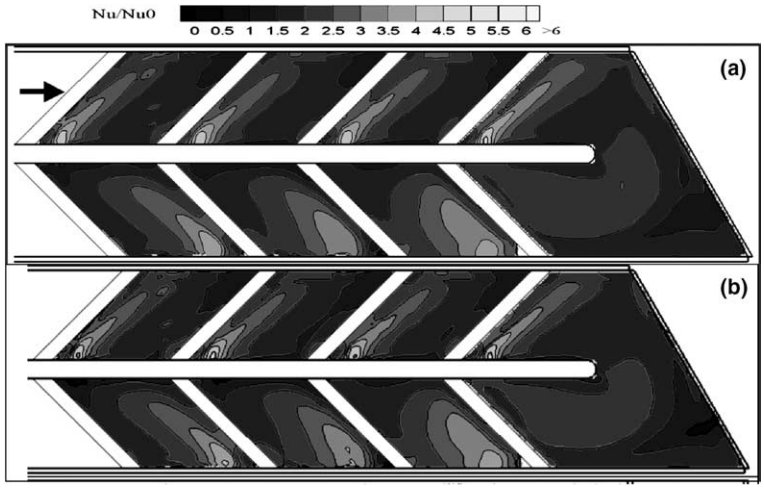

Fig. 12. Heat transfer distribution obtained by the approach using the analytical model (a) and by using the superposition method (b).

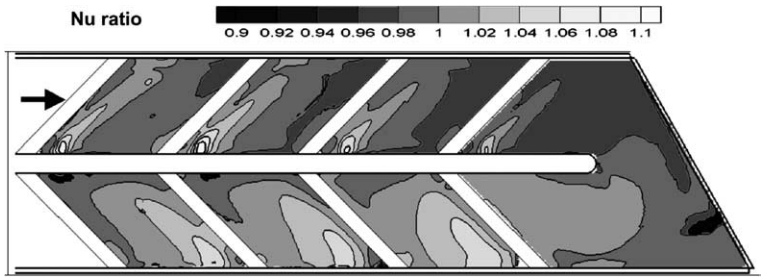

Fig. 13. Ratio of the local heat transfer distribution from the two methods.

compared to the results from the first data evaluation using the measured thermocouple data directly and applying the superposition as given by Eq. (1) in Fig. 12.

As can be seen, both results are very similar. To reveal the differences obtained by the two methods, the ratio of the local heat transfer coefficients is given in Fig. 13. The differences are within 10% with the higher values in the regions of high heat transfer. It should be noted, that a variation of 10% in the heat transfer parameter as shown in Fig. 9 causes a variation of 2–5% in the local heat transfer coefficient using Eq. (8), with the larger values for the higher local heat transfer coefficients. Therefore, the difference can not only be attributed to the uncertainty in the obtained heat transfer parameter. The alternative data evaluation method is thought to base the heat transfer coefficient on a temperature closer to the bulk temperature than the superposition method. This will lead to differences in the obtained data. Nevertheless the difference between both methods is small, which indicates that the flow situation reflects a well-mixed behaviour and that a single thermocouple placed in the mean flow region provides a relatively good estimate for the bulk temperature in this case.

6. Conclusions

A transient heat transfer experiment in a long internal cooling configuration has been analysed. Two methods have been used. The first method uses the measured fluid temperature data at a given location applying the superposition model. The other method analyses the fluid temperature measurements applying a simplified analytical model. This model is used to correct the temperature measurements towards the average value at a given location. This temperature is used for data reduction purposes. It is shown, that both methods lead to similar results for the present application. This reflects the well-mixed flow situation usually found in cooling geometries like the one considered. Differences between the two methods are related to the different fluid temperature histories used for the heat transfer evaluation. The method using a simplified analytical model is thought to base the heat transfer coefficients on a reference temperature closer to the bulk temperature than the first method and should be used for data reduction purposes. Further this method physically analyses the transient thermal situation during the experiments and allows

to easily identify possible erroneous thermocouple measurements.

Acknowledgments

This study was funded by the Swiss Office of Science in cooperation with the Brite Euram Internal Cooling of Turbine Blades project (contract number: BRPR-CT97-0600, project number: BE97-4022). One of the authors (D. Chanteloup) thanks the project partners of this programme for permission to publish this paper.

References

[1] P.T. Ireland, T.V. Jones, Liquid crystal measurements of heat transfer and surface shear stress, Meas. Sci. Technol. 11 (2000) 969–986.

[2] S.V. Ekkad, J.C. Han, A transient liquid crystal thermography technique for gas turbine heat transfer measurements, Meas. Sci. Technol. 11 (2000) 957–968.

[3] S.V. Ekkad, Y. Huang, J.C. Han, Detailed heat transfer distributions in two-pass square channels with rib turbulators and bleed holes, Int. J. Heat Mass Transfer 41 (23) (1998) 3781–3791.

[4] D. Chanteloup, Experimental investigation of heat transfer and flow characteristics in various geometries of 2-pass internal cooling passages of gas turbine airfoils, Ph.D. Thesis, Ecole Polytechnique Fédérale de Lausanne, vol. no. 2670, 2002.

[5] J. Schabacker, PIV investigation of the flow characteristics in an internal coolant passages of gas turbine airfoils with two ducts connected by a sharp 180° bend, Ph.D. Thesis, Ecole Polytechnique Fédérale de Lausanne, vol. no. 1816, 1998.

[6] M. Schnieder, R. Hoecker, J. von Wolfersdorf, Heat transfer and pressure loss in a 180°-turn of a rectangular, rib-roughened two passage channel, ExHFT5, in: Proceedings of the 5th World Conference on Experimental Heat Transfer, Fluid Mechanics and Thermodynamics, Thessaloniki, 2001.

[7] D. Thurman, P. Poinsatte, Experimental heat transfer and bulk air temperature measurements for a multipass internal cooling model with ribs and bleed, ASME J. Turbomach. 123 (2001) 90–96.

[8] S. Mochizuki, A. Murata, M. Fukunaga, Effects of rib arrangements on pressure drop and heat transfer in a rib-roughened channel with a sharp 180° turn, ASME J. Turbomach. 119 (1997) 610–616.

[9] D.E. Metzger, D.E. Larson, Use of melting point surface coatings for local convective heat transfer measurements in rectangular channel flows with 90° turns, ASME J. Heat Transfer 108 (1986) 48–54.

[10] M.K. Chyu, H. Ding, J.P. Downs, A. Van Sutendael, F.O. Soechting, Determination of local heat transfer coefficient based on bulk mean temperature using a transient liquid crystals technique, Exp. Therm. Fluid Sci. 18 (1998) 142–149.

[11] J. von Wolfersdorf, R. Hoecker, C. Hirsch, A data reduction procedure for transient heat transfer measurements in long internal cooling channels, ASME J. Heat Transfer 120 (1998) 314–321.

[12] D.R.H. Gillespie, Z. Wang, P.T. Ireland, T.V. Jones, Detailed measurements of local heat transfer coefficient in the entrance to normal and inclined film cooling holes, ASME J. Turbomach. 118 (1996) 285–290.

[13] C.L.P Tsang, D.R.H. Gillespie, P.T. Ireland, G.M. Dailey, Analysis of transient heat transfer experiments, in: 8th International Symposium on Transport Phenomena and Dynamics of Rotating Machinery ISROMAC-8 Hawaii, 2000.

[14] S. Schubert, S.O. Neumann, B. Weigand, Heat transfer characteristics in a rib roughened two-pass cooling channel with engine near cross-sections: an experimental and numerical study, in: 10th International Symposium on Transport Phenomena and Dynamics of Rotating Machinery ISROMAC-10 Hawaii, 2004.

[15] D. Chanteloup, Y. Juaneda, A. Bölcs, Combined flow and heat transfer measurements in a 2-pass internal coolant passage of gas turbine airfoils, ASME-2002-30214, 2002.

[16] D. Chanteloup, A. Bölcs, Flow effects on the bend region heat transfer distribution of 2-pass internal cooling passages of gas turbine airfoils: influence of film cooling extraction, ASME-2003-38702, 2003.

[17] Z. Wang, D.R.H. Gillespie, P.T. Ireland, Advances in heat transfer measurements using liquid crystals, Turbulent Heat Transfer (Engineering Foundation), 1-25 San Diego, 1996.

[18] R. Hoecker, Optimization of transient heat transfer measurements using thermochromic liquid crystals based on an error estimation, ASME-96-GT-235, 1996.

[19] C.L.P. Tsang, P.T. Ireland, G.M. Dailey, Reduced instrumentation heat transfer testing of model turbine blade cooling systems, in: AVT Symposium on ''Advanced Flow Management'', Loen, Norway, 2001.